

"This accepted author manuscript is copyrighted and published by Elsevier. It is posted here by agreement between Elsevier and MTA. The definitive version of the text was subsequently published in *CHEMICAL PHYSICS LETTERS* 600: pp. 73-78. 25 March 2014, doi: [10.1016/j.cplett.2014.03.050](https://doi.org/10.1016/j.cplett.2014.03.050). Available under license CC-BY-NC-ND."

## Adsorption of H<sub>2</sub>O<sub>2</sub> at the surface of I<sub>h</sub> ice, as seen from grand canonical Monte Carlo simulations

Sylvain Picaud<sup>1</sup> and Pál Jedlovszky<sup>2,3,4</sup>

<sup>1</sup>*Institut UTINAM (CNRS UMR 6213), Université de Franche-Comté, 16 route de Gray, F-25030 Besançon Cedex (France)*

<sup>2</sup>*Laboratory of Interfaces and Nanosize Systems, Institute of Chemistry, Eötvös Loránd University, Pázmány P. Szny 1/A, H-1117 Budapest, Hungary*

<sup>3</sup>*MTA-BME Research Group of Technical Analytical Chemistry, Szt. Gellért tér 4, H-1111 Budapest, Hungary*

<sup>4</sup>*EKF Department of Chemistry, Leányka utca 6, H-3300 Eger, Hungary*

**Running title:** H<sub>2</sub>O<sub>2</sub> Adsorption on Ice

**e-mail:** sylvain.picaud@univ-fcomte.fr (SP), pali@chem.elte.hu (PJ)

### Abstract

Adsorption of H<sub>2</sub>O<sub>2</sub> at the (0001) surface of I<sub>h</sub> ice is investigated by GCMC simulations under tropospheric conditions. The results are in qualitative agreement with experimental data and reveal that the main driving force of the adsorption is the formation of new H<sub>2</sub>O<sub>2</sub>-H<sub>2</sub>O<sub>2</sub> rather than H<sub>2</sub>O<sub>2</sub>-water H-bonds. The isotherm belongs to class III and not even its low pressure part can be described by the Langmuir formalism. At low coverages H<sub>2</sub>O<sub>2</sub> prefers perpendicular alignment to the surface, in which they can form three H-bonds with surface waters. At higher coverages parallel alignment, stabilized by H-bonds between neighbouring H<sub>2</sub>O<sub>2</sub> molecules, becomes increasingly preferred.

## 1. Introduction

It is now widely recognized that ice particles in cirrus ice clouds affect tropospheric chemistry by interacting with gas species, such as acid molecules or volatile organic compounds (VOCs) that can thus be selectively depleted from the gas phase. Moreover, at the surface of ice, chemical or photochemical reactions may occur with significantly different rates from the gas phase, thus modifying the fate of these species in the troposphere [1]. In addition to this role in the troposphere, recent evidence has also shown that the large snow cover in the polar cryosphere can have a major influence on the overlying atmosphere [2]. Snow is a highly photochemically active substrate where the trapped species are efficiently photolyzed, leading to the release of reactive gases into the boundary layer [3]. In both cases (cirrus clouds and snow), one of the central question is to know the degree to which gases partition to the ice surface and to understand the underlying mechanisms. In this way, the importance of gas-to-ice scavenging can be better estimated and the chemical form to which the adsorbed species may transform upon adsorption can be better understood.

In recent years, many experimental and theoretical studies have been devoted to a thorough characterization of the interaction between the surface of ice and a wide variety of atmospheric trace gases [4-14]. Among the information recorded in these works, full adsorption isotherm appears much useful because it gives directly the surface coverage as a function of temperature and partial pressure. In addition to this quantitative information on the uptake importance, these works have also evidenced that computer simulations can very well complement experimental studies in investigating the adsorption of atmospherically relevant molecules at solid surfaces. In particular, computer simulations provide an atomistic level insight into both the three-dimensional structure of the adsorption layer and the energetic of the adsorption process.

The grand canonical Monte Carlo (GCMC) method [15,16] is particularly suitable for this task since in such simulation the chemical potential of the adsorbed molecule is fixed and the number of these molecules is consequently left to fluctuate. Thus, by systematically varying the adsorbate chemical potential in a set of simulations the adsorption isotherm, i.e., the number of adsorbed molecules per surface unit as a function of the chemical potential, can be calculated. The GCMC method has successfully been applied to calculate the adsorption isotherm in a wide variety of such systems [6-9,13,14,17-25], including trace gases on ice [6-9,13,14].

In the present study, we complete this series by focusing on the adsorption of hydrogen peroxide ( $\text{H}_2\text{O}_2$ ) on ice.  $\text{H}_2\text{O}_2$  is present in the global atmosphere in significant volume mixing ratios, varying from tens of ppt (parts per trillion) to a few ppb (parts per billion) [26,27]. This molecule is intimately linked to the important atmospheric cycles that governed the oxidizing properties of the atmosphere through its direct influence on  $\text{HO}_x$  formation and destruction [28]. Indeed, oxidants such as  $\text{HO}_x$  play a key role in environmental chemistry because they react readily with organic pollutants in atmosphere, natural water, ice and snow, transforming these molecules to other chemical forms with different properties and impact [28,29]. The corresponding reactions are not single pathways. They rather form complex cycling reactions which are strongly interconnected [30], and any modification of one of these reactions can influence all the connected processes. For instance,  $\text{H}_2\text{O}_2$  is an important termination products of the  $\text{HO}_x$ ,  $\text{NO}_x$  and VOC cycling reactions (because  $\text{HO}_2 + \text{HO}_2 \rightarrow \text{H}_2\text{O}_2 + \text{O}_2$ ). Its uptake to ice and snow can remove it from the atmosphere and thus directly influence the oxidizing reactions of VOCs.

Despite of this importance, only three experimental studies [4,5,10] have been devoted so far to the characterization of the  $\text{H}_2\text{O}_2$  uptake on ice. Although the two short time scale experiments [5,10] concluded to a reversible adsorption, their results strongly differed regarding the  $\text{H}_2\text{O}_2$  partitioning towards the ice surface. Indeed, the study by Pouvesle et al. [10] proposed a partitioning towards the ice surface two orders of magnitude higher than the study by Clegg and Abbatt [5]. On long time scales, a long term uptake was observed, which is likely related to bulk incorporation [4]. As far as we know, only one theoretical paper has tentatively addressed this topic, based on DFT calculations on small water clusters at 0 K, i.e., a model that is far from representing the complexity of the ice surface under tropospheric conditions [31].

In this paper we thus present GCMC simulations of the adsorption of  $\text{H}_2\text{O}_2$  at the basal surface of  $\text{I}_h$  ice at the atmospherically relevant temperature of 200 K. Besides calculating the adsorption isotherm, the orientation of the adsorbed molecules and their binding energy is also analyzed at various surface coverages. In sec. 2 details of the calculations performed are given. The obtained results concerning the adsorption isotherm and properties of the adsorbed molecules attached to the ice surface are presented and discussed in detail in sec. 3. Finally, in sec. 4 the main conclusions are summarized.

## 2. Grand canonical Monte Carlo simulations

Monte Carlo simulations have been performed on the grand canonical  $(\mu, V, T)$  ensemble at 200 K to model the adsorption of  $\text{H}_2\text{O}_2$  at the (0001) surface of  $\text{I}_h$  ice. The  $X$ ,  $Y$  and  $Z$  edges of the rectangular basic box were 100.0, 35.926 and 38.891 Å, respectively,  $X$  being the axis perpendicular to the ice surface. The basic box contained 2880 water molecules, whereas the chemical potential of  $\text{H}_2\text{O}_2$ ,  $\mu$ , has been fixed and the number of  $\text{H}_2\text{O}_2$  molecules has been left to fluctuate. In the entire set of 23 simulations the range of chemical potential between -77.33 and -40.75 kJ/mol has been explored in steps of 1.66 kJ/mol.

The water molecules have been described by the TIP5P potential [32] since this model has been shown to reproduce well the melting point of  $\text{I}_h$  ice. [33]  $\text{H}_2\text{O}_2$  molecules have been modelled by the potential proposed by Vácha et al., originally developed to describe the adsorption of  $\text{H}_2\text{O}_2$  at the surface of liquid water. [34] All molecules have been kept rigid; the intermolecular interactions have been truncated to zero beyond a molecule centre-based cut-off distance of 12.5 Å.

The simulations have been performed using the program MMC. [35] In a Monte Carlo step either a randomly chosen molecule has been randomly translated and rotated by no more than 0.25 Å and  $15^\circ$ , respectively, or a  $\text{H}_2\text{O}_2$  molecule has been either randomly inserted to, or removed from, the system. Particle displacement and insertion/deletion steps have been made in an alternating order, insertions and deletions have been attempted with equal probabilities. For the insertion/deletion attempts the cavity biased scheme of Mezei has been used. [36,37] Cavities with a minimum radius of 2.5 Å have been searched for in a  $100 \times 100 \times 100$  grid. At least 10% of the particle displacement and 0.5% of the insertion/deletion attempts have turned out to be successful in every simulation.

All simulations have been started from the perfect  $\text{I}_h$  crystal structure with water molecules arranged in 18 molecular layers along the surface normal axis  $X$ , and two  $\text{H}_2\text{O}_2$  molecules randomly placed in the vapour phase. The systems have been equilibrated by performing  $3 \times 10^8$  -  $3 \times 10^9$  Monte Carlo steps, depending on how slowly the number of the  $\text{H}_2\text{O}_2$  molecules in the box converged. Once the number of  $\text{H}_2\text{O}_2$  molecules started to fluctuate, its mean value has been evaluated by averaging over  $2 \times 10^8$  equilibrium configurations. Finally, at selected chemical potential values 2500 sample configurations, separated by  $2 \times 10^5$  Monte Carlo steps each, have been saved for further analyses.

### 3. Results and Discussion

The adsorption isotherm of  $\text{H}_2\text{O}_2$  on ice obtained from our simulations is shown in Figure 1. As is seen, an increase of the  $\text{H}_2\text{O}_2$  chemical potential leads to a continuous increase of the number of adsorbed molecules; no plateau corresponding to a particularly stable adsorption layer is seen. Above a  $\mu$  value of about  $-52$  kJ/mol the space between the two ice surfaces in the simulation box is completely filled by  $\text{H}_2\text{O}_2$  molecules. However, unlike for several other adsorbates, [6,14] this filling of the box does not occur as a sharp transition, indicating that it is probably due to the fact that the adsorption layer of  $\text{H}_2\text{O}_2$  simply reaches the thickness of the vapour phase in the basic box rather than due to the condensation of  $\text{H}_2\text{O}_2$ . To confirm this assumption and determine the real, finite size effect error-free point of condensation of  $\text{H}_2\text{O}_2$  we have repeated the GCMC simulations without the ice slab in the basic box. [25] In this case condensation of  $\text{H}_2\text{O}_2$  occurred as a very sharp transition at the  $\mu$  value of  $-38.670$  kJ/mol. This value is considerably larger than that corresponding to the filling of the vapour phase in the basic box of about  $-52$  kJ/mol, indicating that the adsorption layer of  $\text{H}_2\text{O}_2$  can be even several orders of magnitude thicker than the distance of  $\sim 40$  Å of the two ice surfaces in the basic box. In other words, the thickness of the adsorption layer can well fall in the mesoscopic or, perhaps, even to the macroscopic size range. Among the contradicting experimental data, our finding thus clearly supports the results of Pouvelse et al. [10] rather than those of Clegg and Abbatt [5], who found surprisingly low affinity of  $\text{H}_2\text{O}_2$  to ice.

Based on the behaviour of the adsorption isotherm we have collected sample configurations for further analyses at five different chemical potential values, namely at  $-72.3$ ,  $-65.7$ ,  $-59.0$ ,  $-55.7$  and  $-54.1$  kJ/mol. These systems, also indicated in Fig. 1, are referred to here as systems I-V, respectively. An equilibrium snapshot of the adsorption layer in these systems is shown in Figure 2.

The number density profile of the  $\text{H}_2\text{O}_2$  molecules along the surface normal axis in systems I-V is shown in Figure 3. For reference, the density profile of the outmost layer of ice is also shown. As is seen, the increase of the chemical potential leads to a simultaneous increase of the height of the first peak around  $33.5$  Å, corresponding to the first molecular layer of  $\text{H}_2\text{O}_2$  and to the development and thickening of the outer layer of the  $\text{H}_2\text{O}_2$  molecules. Thus, similarly to the adsorption layer of water at various polar surfaces [20,23,25], the outer molecular layer of  $\text{H}_2\text{O}_2$  starts to develop well before the first layer, being in contact with the ice surface, gets saturated. As a consequence, not even the low pressure part of the adsorption

isotherm can be described in terms of the Langmuir formalism. This finding is in accordance with the experimental results of Pouvelse et al., who observed a continuous increase of the adsorption isotherm, without convergence to a saturation value [10]. Fitting the functional form of the Langmuir isotherm to the data up to the point where traces of the outer layer appear can, on the other hand, be used to estimate the saturation density of the first molecular layer. Performing this fit up to the chemical potential value of  $-65.7$  kJ/mol resulted in the saturation density value of  $6.3 \mu\text{mol}/\text{m}^2$ , again in a good agreement with the experimental result of Pouvelse et al. of  $6.6 \mu\text{mol}/\text{m}^2$  [10]. The observed development of the subsequent molecular layers also suggests that lateral interactions are probably stronger in the adsorption layer than the adsorbate-ice interaction, and hence the adsorption isotherm belongs to class III according to IUPAC convention.

To confirm this assumption we have calculated the distribution of the binding energy,  $U_b$ , of the  $\text{H}_2\text{O}_2$  molecules of the first molecular layer at the ice surface. (The outer boundary of this layer has been set to  $X = 35 \text{ \AA}$ , i.e., to the position of the density minimum following the first peak, see Fig. 3).  $U_b$  is simply the interaction energy of an adsorbed  $\text{H}_2\text{O}_2$  molecule with the rest of the system. Besides the total binding energy, the distribution of the contributions due to the lateral and to the ice-adsorbate interaction,  $U_b^{\text{lat}}$  and  $U_b^{\text{ice}}$ , respectively, have also been calculated. The binding energy distributions obtained in systems I, II, III and V are shown in Figure 4. (The results in system IV turned out to be very similar to those in system V.)

The  $P(U_b^{\text{ice}})$  distribution exhibits its main peak around  $-75$  kJ/mol. Considering that the interaction energy of a H-bonded water pair is around  $-25$  kJ/mol, this value suggests the formation of three hydrogen bonds between an adsorbed  $\text{H}_2\text{O}_2$  molecule and the ice surface. At very low coverages a small fraction of the molecules can even form four or five hydrogen bonds with ice, as evidenced by the small peak of system I below  $-100$  kJ/mol. More importantly, at higher coverages another peak of  $P(U_b^{\text{ice}})$  emerges around  $-20$  kJ/mol. In system III this peak is already very pronounced and when the first molecular layer gets saturated it becomes as high as the other peak at lower energies. The development of this peak evidences an increasing fraction of the first layer  $\text{H}_2\text{O}_2$  molecules that form a single hydrogen bond with the ice phase.

Simultaneously with the decrease of the magnitude of  $U_b^{\text{ice}}$ , the lateral contribution to the binding energy becomes more important. The  $P(U_b^{\text{lat}})$  distribution exhibits several peaks, separated by about 25 kJ/mol from each other, corresponding to  $\text{H}_2\text{O}_2$  molecules forming different number of H-bonds with their  $\text{H}_2\text{O}_2$  neighbours. It is also clear that in system III, i.e., in the presence of the outer layer of the adsorbed molecules, the lateral contribution to the binding energy already exceeds, on the average, that of the ice-adsorbate interaction, as the majority of the  $\text{H}_2\text{O}_2$  molecules have two or three H-bonded lateral neighbours. Furthermore, in systems IV and V the  $\text{H}_2\text{O}_2$  molecules form three or four H-bonds with other  $\text{H}_2\text{O}_2$  molecules. Thus, the main driving force of the adsorption is clearly the formation of new H-bonds between the adsorbed molecules rather than between  $\text{H}_2\text{O}_2$  and water molecules at the ice surface.

To analyze the preferred orientation of the  $\text{H}_2\text{O}_2$  molecules of the first molecular layer relative to the ice surface we have calculated the bivariate distribution of  $\cos\vartheta$  and  $\phi$ ,  $\vartheta$  and  $\phi$  being the polar angles of the surface normal vector,  $\underline{X}$ , pointing away from the ice phase, in a coordinate frame fixed to the individual  $\text{H}_2\text{O}_2$  molecules [38,39]. The definition of this local frame and of the polar angles  $\vartheta$  and  $\phi$  is shown in Figure 5. Thus, axis  $\underline{x}$  of the local frame points along the O-O bond of the  $\text{H}_2\text{O}_2$  molecule, axis  $\underline{z}$  is the molecular normal, and axis  $\underline{y}$  is perpendicular to  $x$  and  $z$ .

The  $P(\cos\vartheta, \phi)$  orientational maps obtained in systems I, II, III and V are shown in Figure 5. (Again, results in system IV turned out to be very similar to those in system V.) As seen, the orientation corresponding to  $\cos\vartheta = 0$  and  $\phi = 90^\circ$ , denoted as A, dominates the map in every case, however, the strength of this orientational preference decreases with increasing surface coverage. In this orientation the  $\text{H}_2\text{O}_2$  molecule stays perpendicular to the ice surface, while its O-O axis is parallel with the surface plane (see Fig. 5). In this orientation the  $\text{H}_2\text{O}_2$  molecule is able to form three H-bonds with surface water molecules, the latter also aligned in one of their preferred orientations [6], as illustrated in Figure 6. Further, simultaneously with the building up of the outer molecular layers of  $\text{H}_2\text{O}_2$ , another preferred orientation of the  $\text{H}_2\text{O}_2$  molecules, corresponding to  $\cos\vartheta = 1$ , develops. In this orientation, marked as B, the  $\text{H}_2\text{O}_2$  molecule lays parallel with the ice surface (see Fig. 5), and cannot form more than two H-bonds with the surface water molecules. On the other hand, in accordance with the binding energy distributions, these molecules of orientation B can easily form three or, in case of a slight tilt from the exactly parallel alignment, even four H-bonds with their  $\text{H}_2\text{O}_2$  neighbours,

some of which belonging to the outer molecular layer. Possible H-bond formations of a  $\text{H}_2\text{O}_2$  molecule of orientation B are also depicted in Fig. 6.

#### 4. Summary and Conclusions

In this paper we presented a detailed analysis of the adsorption of  $\text{H}_2\text{O}_2$  at the (0001) surface of  $\text{I}_h$  ice by means of GCMC computer simulations. Our results indicated, in accordance with the experimental data of Pouvelse et al. [10] but in contrast to those of Clegg and Abbatt [5], a high affinity of  $\text{H}_2\text{O}_2$  to ice. The main thermodynamic driving force of the adsorption turned out to be the formation of new H-bonds between the adsorbed  $\text{H}_2\text{O}_2$  molecules rather than between  $\text{H}_2\text{O}_2$  and surface water molecules. As a consequence, not even the low pressure part of the adsorption isotherm can be described in terms of the Langmuir approximation; the adsorption isotherm belongs to class III according to the IUPAC convention. The adsorption layer can be surprisingly thick, reaching at least the mesoscopic size range. This result, being also compatible with the experimental findings of Pouvelse et al. [10], implies that in the upper troposphere  $\text{H}_2\text{O}_2$ , in concentrations not higher than a few ppb [26] may even fully be adsorbed at the surface of the ice grains.

**Acknowledgements.** This project is supported by the Hungarian OTKA Foundation under project No. 104234 and by the CNRS in the framework of an international program for scientific cooperation (PICS). P. J. is a Szentágothai János fellow of Hungary, supported by the European Union, co-financed by the European Social Fund in the framework of TÁMOP 4.2.4.A/2-11/1-2012-0001 “National Excellence Program” under grant number A2-SZJÖ-TOK-13-0030.



## References

- [1] J. P. D. Abbatt, *Chem. Rev.* 103 (2003) 4783.
- [2] F. Dominé and P. B. Shepson, *Science* 297 (2002) 1506.
- [3] A. M. Grannas, A. E. Jones, J. Dibb, M. Ammann, C. Anastasio, H. J. Beine, M. Bergin, J. Bottenheim, C. S. Boxe, G. Carver et al., *Atmos. Chem. Phys.* 7 (2007) 4329.
- [4] M. H. Conklin, A. Sigg, A. Neftel, and R. C. Bales, *J. Geophys. Research-Atmospheres* 98 (1993) 18367.
- [5] S. M. Clegg, J. P. D. Abbatt, *J. Phys. Chem. A* 105, (2001) 6630.
- [6] P. Jedlovszky, L. Pártay, P. N. M. Hoang, S. Picaud, P. von Hessberg, J. Crowley, *J. Am. Chem. Soc.* 128 (2006) 15300.
- [7] G. Hantal, P. Jedlovszky, P.N.M. Hoang and S. Picaud, *Phys. Chem. Chem. Phys.* 10 (2008) 6369.
- [8] P. Jedlovszky, G. Hantal, K. Neurohr, S. Picaud, P.N.M. Hoang, P. von Hessberg, and J. Crowley, *J. Phys. Chem. C* 112 (2008) 8976.
- [9] M. Petitjean, G. Hantal, C. Chauvin, P. Mirabel, S. Le Calvé, P.N.M. Hoang, S. Picaud, P. Jedlovszky, *Langmuir* 26 (2010) 9596.
- [10] N. Pouvelse, M. Kippenberger, G. Schuster, J. N. Crowley, *Phys. Chem. Chem. Phys.* 12 (2010) 1554.
- [11] J. N. Crowley, M. Ammann, R. A. Cox, R. G. Hynes, M. E. Jenkin, A. Mellouki, M. J. Rossi, J. Troe, and T. J. Wallington, *Atmos. Chem. Phys.* 10 (2010) 9059.
- [12] T. Bartels-Rausch, V. Bergeron, J. H. E. Cartwright, R. Escribano, J. L. Finney, H. Grothe, P. J. Gutiérrez, J. Haapala, W. F. Kuhs, J. B. C. Pettersson et al. *Rev. Modern Phys.* 84 (2012) 885.
- [13] M. Darvas, J. Lasne, C. Laffon, P. Parent, S. Picaud, and P. Jedlovszky, *Langmuir* 28 (2012) 4198.
- [14] Zs. E. Mészár, Gy. Hantal, S. Picaud, P. Jedlovszky, *J. Phys. Chem. C* 117 (2013) 6719.
- [15] D. J. Adams, *Mol. Phys.* 29 (1975) 307.
- [16] M. P. Allen, D. J. Tildesley, *Computer Simulation of Liquids*, Clarendon, Oxford, 1987.
- [17] R. J. M. Pellenq, B. Tavittian, D. Espinat, A. H. Fuchs, *Langmuir* 12 (1996) 4768.

- [18] E. A. Muller, F. R. Hung, K. E. Gubbins, *Langmuir* 16 (2000) 5418.
- [19] C. D. Daub, G. N. Patey, D. B. Jack, A. K. Sallabi *J. Chem. Phys.* 124 (2006) 114706.
- [20] F. Moulin, S. Picaud, P. N. M. Hoang, P. Jedlovszky, *J. Chem. Phys.* 127 (2007) 164719.
- [21] G. Garberoglio, *Langmuir* 23 (2007) 12154.
- [22] G. Rutkai, T. Kristóf, *Chem. Phys. Lett.* 462 (2008) 269.
- [23] E. Tombácz, A. Hajdú, E. Illés, K. László, G. Garberoglio, P. Jedlovszky, *Langmuir* 25 (2009) 13007.
- [24] T. Croteau, A. K. Bertram, G. N. Patey, *J. Phys. Chem. A* 113, (2009) 7826.
- [25] M. Szóri, M. Roeselová, P. Jedlovszky, *J. Phys. Chem. C* 115 (2011) 19165.
- [26] M. H. Lee, B. G. Heikes and D. W. O'Sullivan, *Atmos. Environ.* 34 (2000) 3475.
- [27] N. D. C. Allen, G. G. Abad, P. F. Bernath, and C. D. Boone, *J.Q.S.R.T.* 115 (2013) 66.
- [28] J. H. Seinfeld and S. N. Pandis. *Atmospheric Chemistry and Physics: from air pollution to climate change* (John Wiley & Sons, New York, 1998)
- [29] T. F. Dahan, R. Zhao, D.J. Donaldson, *Atmos. Chem. Phys.* 10 (2010) 843.
- [30] R. Atkinson, *Atmos. Environ.* 34 (2000) 2063.
- [31] S. K. Ignatov, A. G. Razuvaev, P. G. Sennikov, O. Schrems, *J. Mol. Struct. THEOCHEM* 908 (2009) 47.
- [32] M. Mahoney, W. L. Jorgensen, *J. Chem. Phys.* 112 (2000) 8910.
- [33] C. Vega, E. Sanz, J. L. F. Abascal, *J. Chem. Phys.* 122 (2005) 114507.
- [34] R. Vácha, P. Slavíček, M. Mucha, B. J. Finnlayson-Pitts, P. Jungwirth, *J. Phys. Chem. A* 108, (2004) 11573.
- [35] M. Mezei, M. MMC: Monte Carlo Program for Simulation of Molecular Assemblies. URL: <http://inka.mssm.edu/~mezei/mmc>.
- [36] M. Mezei, *Mol. Phys.* 40 (1980) 901.
- [37] M. Mezei, *Mol. Phys.* 61 (1987) 565, erratum: *Mol. Phys.* 67 (1989) 1207.
- [38] P. Jedlovszky, Á. Vincze, G. Horvai, *J. Chem. Phys.* 17 (2002) 2271.
- [39] P. Jedlovszky, Á. Vincze, G. Horvai, *Phys. Chem. Chem. Phys.* 6 (2004) 1874.

## Figure legends

Fig.1. Adsorption isotherm of  $\text{H}_2\text{O}_2$  on  $\text{I}_h$  ice, as obtained from our simulations. The line connecting the points is just a guide to the eye. The state points corresponding to systems I-V are marked by arrows.

Fig. 2. Instantaneous equilibrium snapshots of systems I-V, in side view (top row) and top view (bottom row). Water O atoms are shown as blue dots,  $\text{H}_2\text{O}_2$  O and H atoms are shown by red and white colorurs, respectively. Water H atoms are omitted for clarity.

Fig.3. Number density profile of  $\text{H}_2\text{O}_2$  along the surface normal axis  $X$  in systems I-V. The water number density profile in system I is also shown for the outmost ice layer, and, in the inset, also for the entire system. All profiles shown are symmetrized over the two interfaces in the basic box. The dotted vertical line marks the outer boundary of the first layer of adsorbed  $\text{H}_2\text{O}_2$  molecules.

Fig. 4. Distribution of the total binding energy of the first layer  $\text{H}_2\text{O}_2$  molecules,  $U_b$  (bottom); its contributions coming from the other  $\text{H}_2\text{O}_2$  molecules (middle) and from the ice phase (top), as obtained in systems I, II, III and V.

Fig. 5. Orientational map of the first layer  $\text{H}_2\text{O}_2$  molecules in systems I, II, III and V. Lighter colors indicate higher probabilities. The definition of the local Cartesian frame fixed to the individual  $\text{H}_2\text{O}_2$  molecules (top) as well as the two preferred alignments of  $\text{H}_2\text{O}_2$  (bottom) are also shown.  $\underline{X}$  is the surface normal vector pointing away from the ice phase.

Fig. 6. Possible H-bonds between a surface  $\text{H}_2\text{O}_2$  molecule (a) in its preferred alignment A and three water molecules of the ice surface, (b) in its preferred alignment B and two water molecules of the ice surface, and (c) in its preferred alignment B and four other surface  $\text{H}_2\text{O}_2$  molecules, also aligned in orientation B. The water orientations correspond to preferred alignments at the ice surface [6]. O and H atoms are depicted by red and white spheres, respectively, whereas the H-bonds are marked by thick dotted lines. The plane of the ice surface is also indicated.



**Figure 1.**  
**Picaud and Jedlovszky**

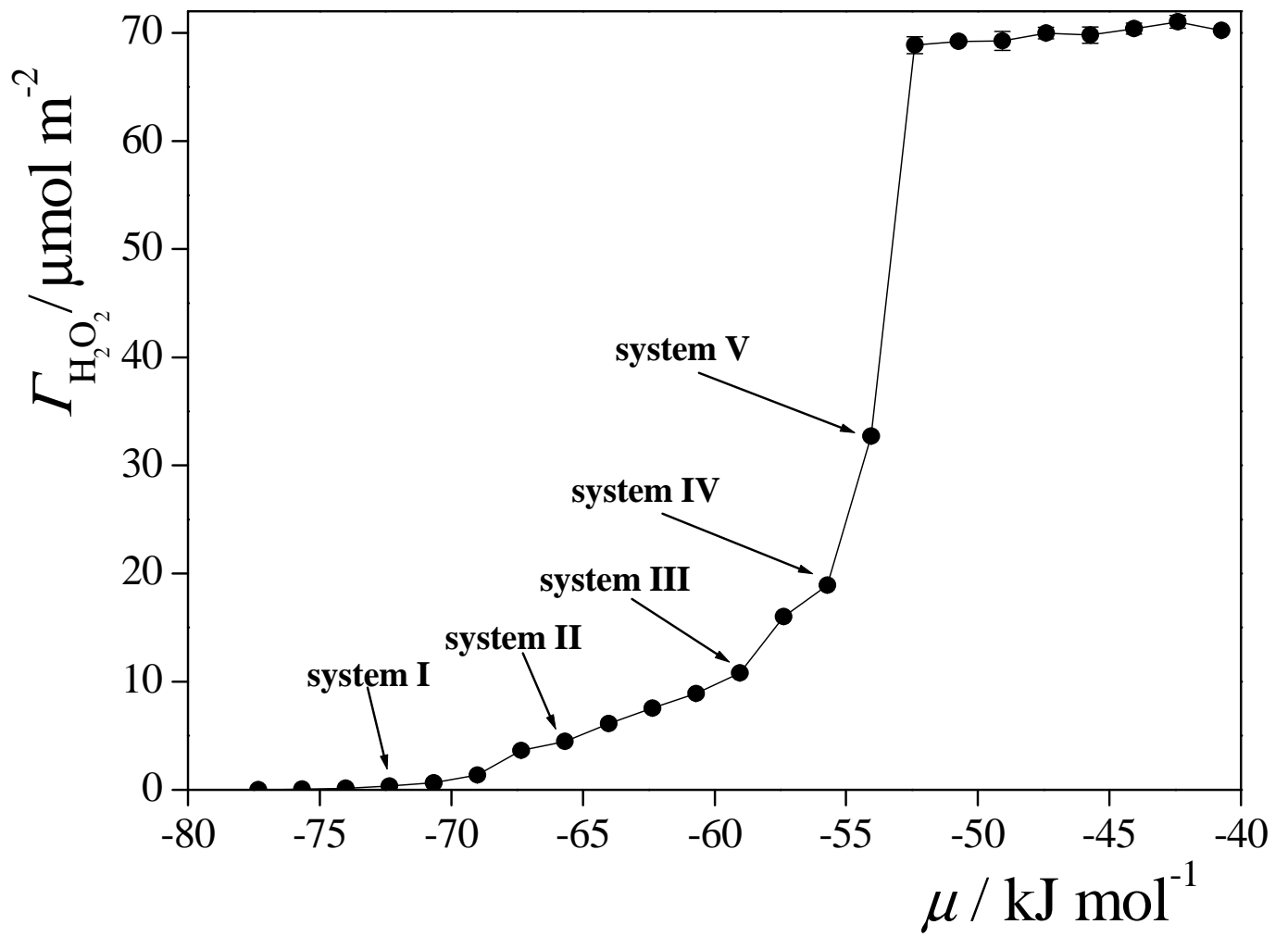
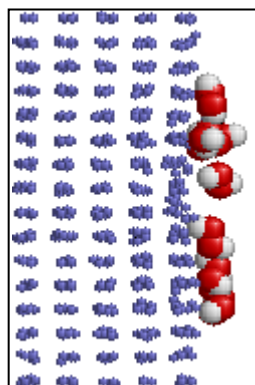
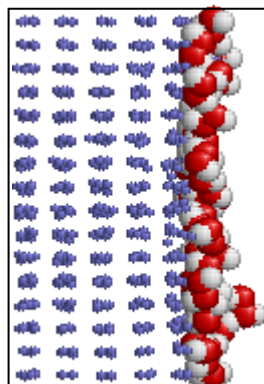


Figure 2.  
Picaud and Jedlovsky

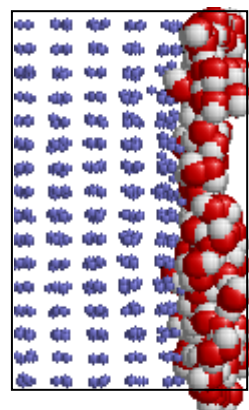
system I



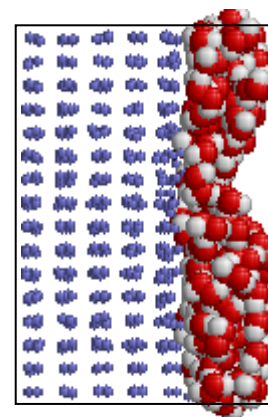
system II



system III



system IV



system V

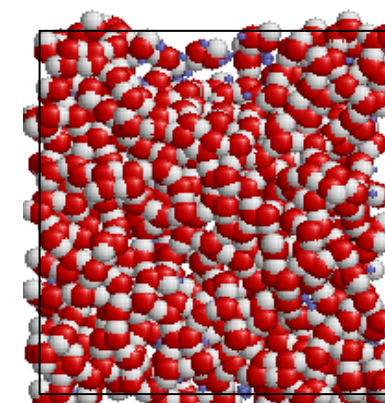
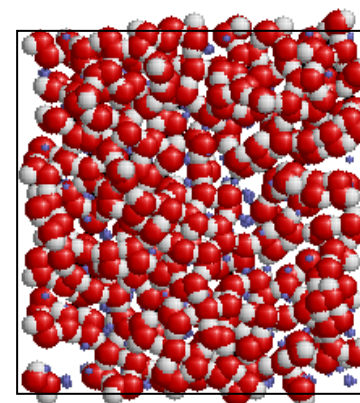
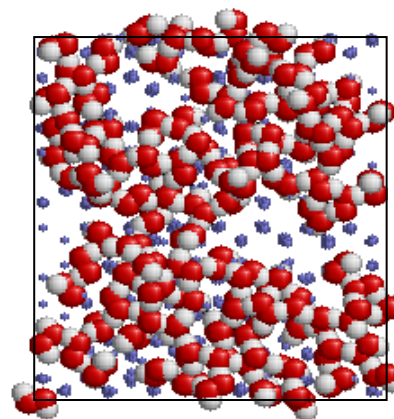
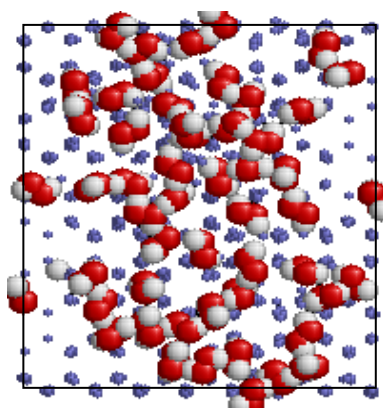
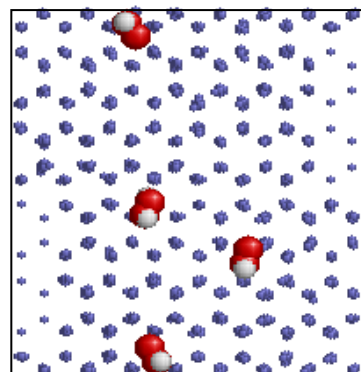
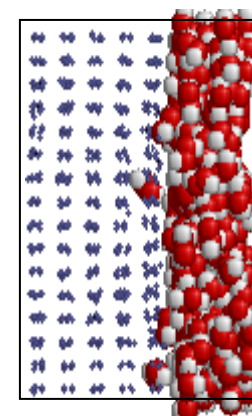


**Figure 3.**  
**Picaud and Jedlovszky**

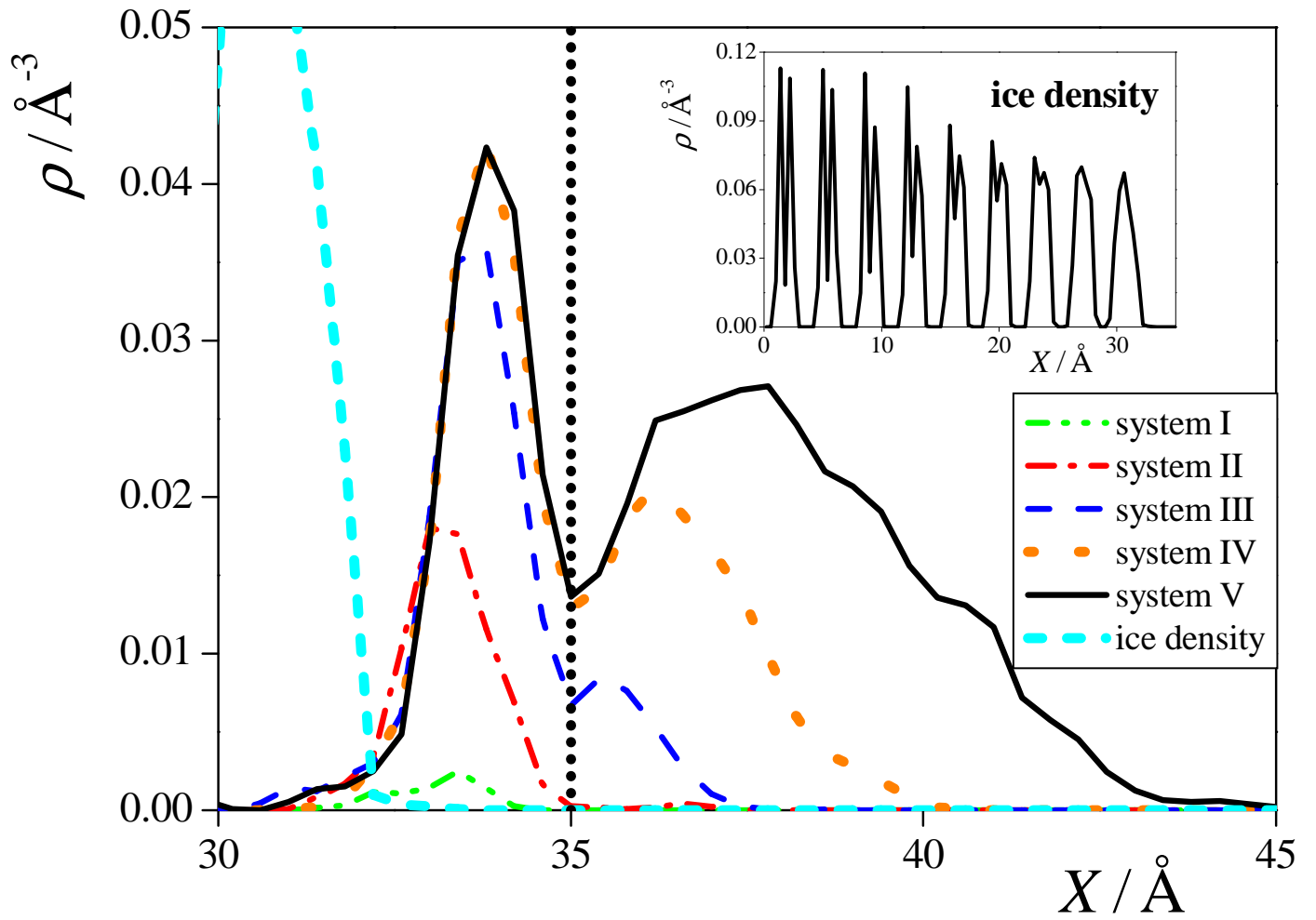
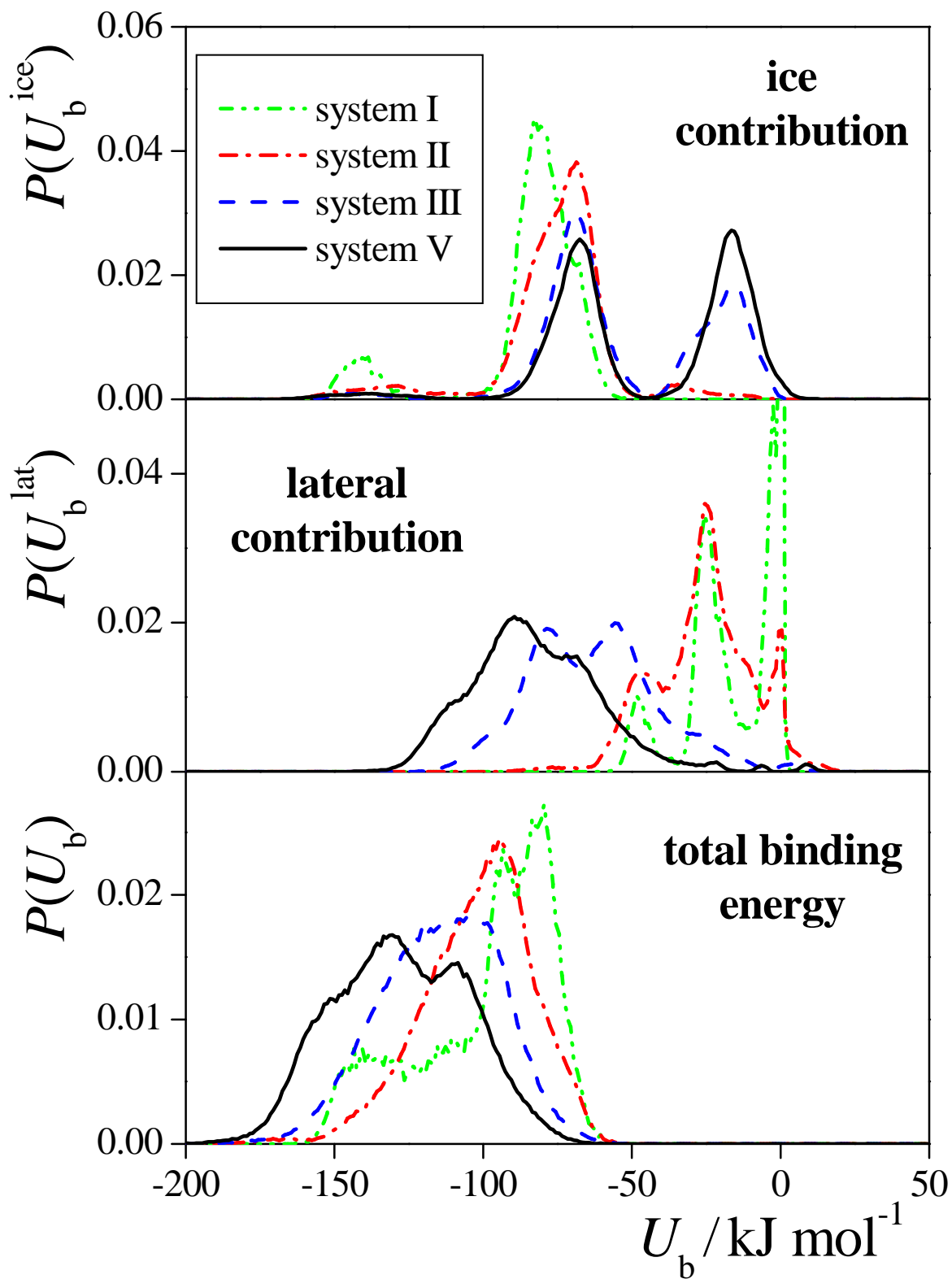
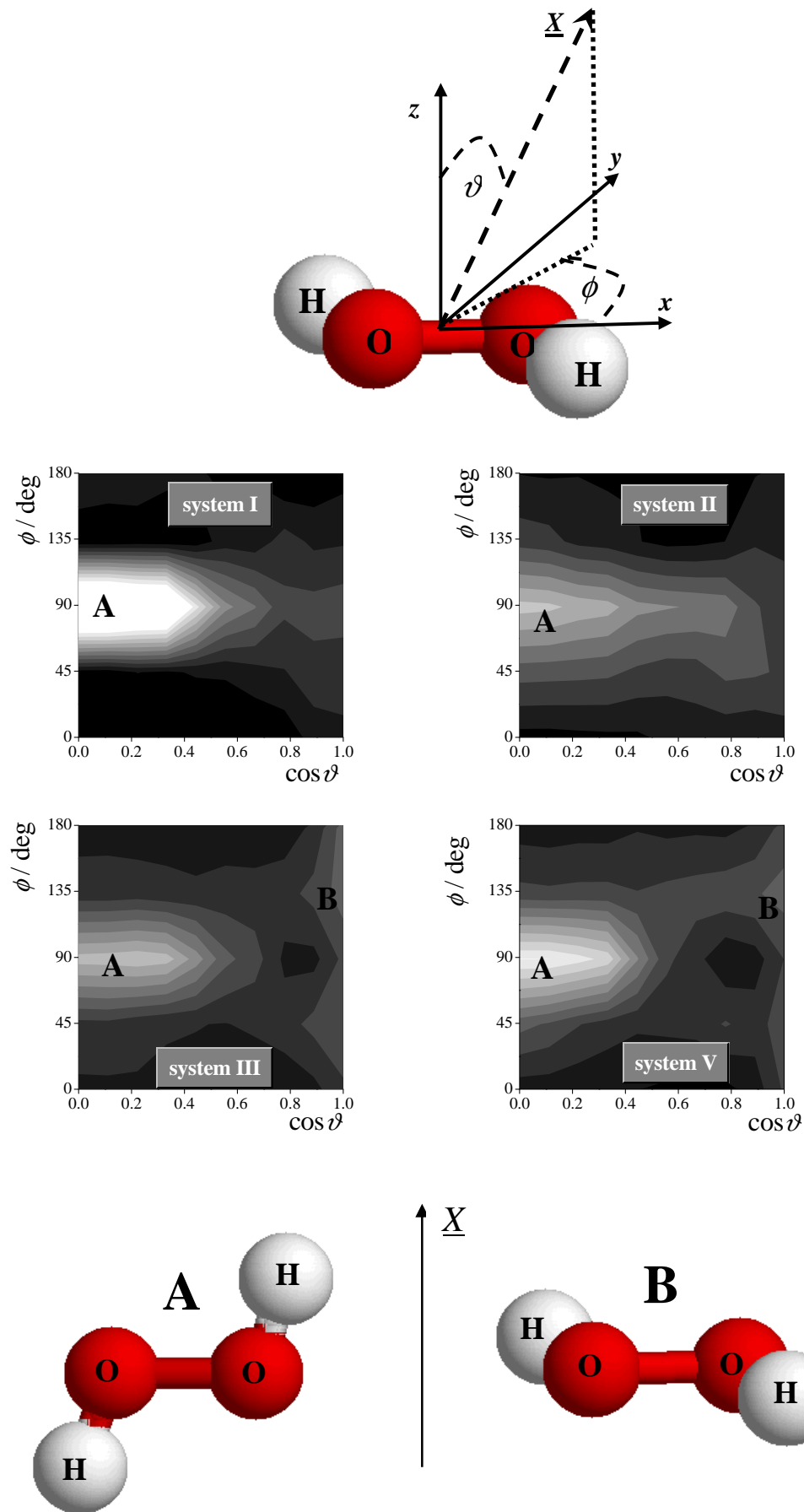


Figure 4.  
Picaud and Jedlovsky

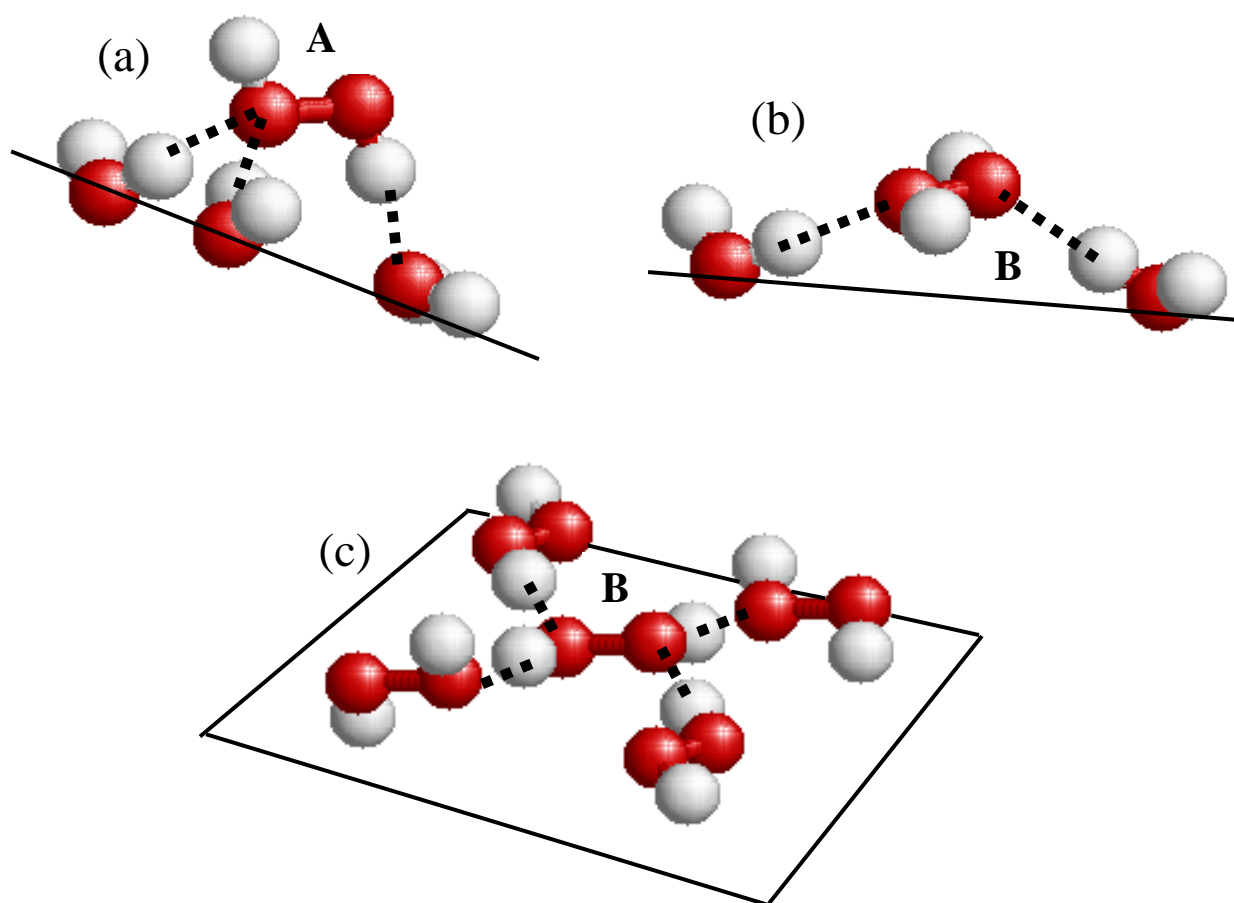




**Figure 5.**  
Picaud and Jedlovsky



**Figure 6.**  
**Picaud and Jedlovsky**



## Graphical abstract

Properties of the adsorption layer of  $\text{H}_2\text{O}_2$  on  $\text{I}_h$  ice is compared at various coverages under tropospheric conditions.

